Proc. Natl. Acad. Sci. USA
Vol. 93, pp. 13280–13285, November 1996
Neurobiology

Functional breakdown of the lipid bilayer of the myelin membrane in central and peripheral nervous system by disrupted galactocerebroside synthesis

(ceramide galactosyl transferase/*cgt* null allele/conduction velocity/dysmyelinosis)

ANDREAS BOSIO, ERIKA BINCZEK, AND WILHELM STOFFEL*

Institute of Biochemistry I, Medical Faculty, University of Cologne, Joseph-Stelzmann-Strasse 52, D-50931 Cologne, Germany

Communicated by Richard M. Krause, National Institutes of Health, Bethesda, MD, July 20, 1996 (received for review June 12, 1996)

ABSTRACT **The lipid bilayer of the myelin membrane of the central nervous system (CNS) and the peripheral nervous system (PNS) contains the oligodendrocyte- and Schwann cell-specific glycosphingolipids galactocerebrosides (GalC) and GalC-derived sulfatides (sGalC). We have generated a UDP-galactose ceramide galactosyltransferase (CGT) null mutant mouse ($cgt^{-/-}$) with CNS and PNS myelin completely depleted of GalC and derived sGalC. Oligodendrocytes and Schwann cells are unable to restore the structure and function of these galactosphingolipids to maintain the insulator function of the membrane bilayer. The velocity of nerve conduction of homozygous $cgt^{-/-}$ mice is reduced to that of unmyelinated axons. This indicates a severely altered ion permeability of the lipid bilayer. GalC and sGalC are essential for the unperturbed lipid bilayer of the myelin membrane of CNS and PNS. The severe dysmyelinosis leads to death of the $cgt^{-/-}$ mouse at the end of the myelination period.**

Axons in the central nervous system (CNS) and the peripheral nervous system (PNS) are ensheathed by oligodendrocyte and Schwann cell plasma membrane processes which assemble the multilayered myelin membrane. The lipid bilayer lends myelin the insulator function in the internodes of axons allowing saltatory conduction. It contains the myelin-specific glycosphingolipids galactocerebrosides (GalCs) and GalC-derived sulfatides (sGalCs). GalC is synthesized by UDP-galactose ceramide galactosyltransferase (CGT). We have studied the function of GalC and sGalC in a CGT-deficient mouse line completely lacking GalC and sGalC in CNS and PNS myelin lipid bilayer. The conduction velocity of myelinated axons of $cgt^{-/-}$ mice is reduced to that of unmyelinated axons indicating a block of saltatory conduction. The impaired insulator function of myelin due to the lack of the main glycolipids GalC and sGalC is not compensated by other lipids. The dysmyelinosis leads to body tremor, loss of locomotor activity, and to death at the end of myelination.

CGT has recently been isolated from rat brain and characterized (1, 2). The coding sequence of human *cgt* on chromosome 4q26 as well as mouse *cgt* is distributed over five exons (3, 4). Oligodendrocytes of CNS, Schwann cells in PNS, and, very weakly, kidney cells show a peak expression of the CGT gene during the myelination period between p10 and p30 (1). GalC serves as an early epitope in oligodendrocyte lineage studies (5–9).

Beyond structural functions complex sphingolipids have been proposed as precursors of second messenger systems in cell signaling and in the differentiation of oligodendrocytes (ref. 10; for a review, see ref. 11).

The publication costs of this article were defrayed in part by page charge payment. This article must therefore be hereby marked "*advertisement*" in accordance with 18 U.S.C. §1734 solely to indicate this fact.

MATERIALS AND METHODS

$cgt^{-/-}$ Replacement Vector. A 7-kb *Sac*I fragment with exon I flanked by 3-kb upstream and 3-kb downstream sequences of the recently described mouse CGT gene (3) was subcloned into pBluescript and used for preparation of the targeting construct. The blunt end 1.2-kb *neo* gene (12) was inserted into the unique *Kpn*I site of exon I at position 72 of the open reading frame in sense direction of the CGT gene fragment. The *tk* gene was ligated as an *Xho*I/*Bam*HI fragment into the *Not*I site of the pBluescript multiple cloning site located at the 5′ end of the CGT gene fragment. The construct was linearized with *Spe*I in the multiple cloning site of pBluescript, Fig. 1*A*.

Generation of $cgt^{-/-}$ Mouse Line. A total of 10^7 R1 cells [(129/j × 129sv-cp)F_1 background] (kindly provided by A. Nagly, Mount Sinai Hospital, Samuel Lunenfeld Research Institute, Toronto) were transfected by electroporation with 20 μg of the linearized targeting vector at 250 V and 500 μF using a Bio-Rad gene pulser. Homologous recombinant clones were selected by adding G418 (300 μg/ml) and gancyclovir (0.2 mM) to the medium. C57BL/6 blastocysts were injected with five R1-independent embryonic stem (ES) cell lines (13). Chimeric males were intercrossed with C57BL/6 mice. Heterozygous offsprings were intercrossed and homozygous $cgt^{-/-}$ mice were obtained in the F2 generation. ES cell clones and tail DNA were prepared according to Laird (14). C57BL/6 wild-type (wt) mice served as control animals in all comparative experiments.

Analysis of RNA Expression. RNA was isolated by the guanidinium thiocyanate-phenol method (15). 25 μg total RNA of brain, kidney, liver, spleen and total RNA of eight sciatic nerves from 18- to 20-day-old wt, $cgt^{+/-}$, and $cgt^{-/-}$ was fractionated by electrophoresis on formaldehyde (1.5%) agarose gels, blotted onto nitrocellulose (GeneScreen, DuPont), and hybridized with randomly ^{32}P-labeled probes. cDNA probes included a 1180-bp *Eco*RI/*Nco*I rat CGT cDNA fragment (3), a 640-bp *Pst*I rat fragment of myelin basic protein (MBP) cDNA encoding the 14.5 kDa isoform of MBP, a 1362-bp *Pst*I fragment of human PLP cDNA, a 206-bp myelin-associated glycoprotein (MAG) genomic DNA fragment of mouse exon IX, a 356-bp DNA fragment of exon I of mouse oligodendrocyte myelin glycoprotein (OMgp), and a 500-bp mouse cDNA fragment of P_0. Glyceraldehyde-phosphate dehydrogenase cDNA was used as internal standard. Signals were recorded with a PhosphorImager (Molecular Dynamics).

For *in situ* hybridization, ^{35}S-labeled RNA probes were prepared by *in vitro* transcription of the 3.5-kb CGT cDNA in

Abbreviations: CNS, central nervous system; PNS, peripheral nervous system; GalC, galactocerebroside; sGalC, GalC-derived sulfatides; CGT, ceramide galactosyltransferase; MBP, myelin basic protein; wt, wild type; MAG, myelin-associated glycoprotein; ES cell, embryonic stem cell; OMgp, oligodendrocyte myelin glycoprotein; PLP, proteolipid protein.

*To whom reprint requests should be addressed. e-mail: Wilhelm.Stoffel@rs1.rrz.uni-koeln.de.

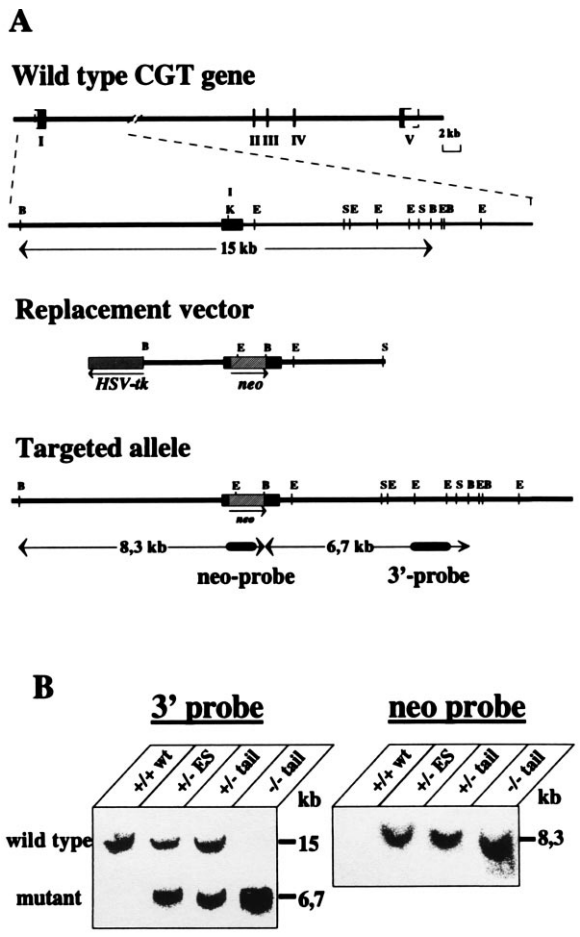

FIG. 1. Disruption of the *cgt* locus in mouse ES cells and generation of CGT-deficient mice. (*A*) Targeting strategy: the murine *cgt*-coding exon I is indicated by a closed box. The neo^r cassette inserted into the *Kpn*I site of exon I and the HSV-tk gene (▨) has been placed upstream of the exon I. B, *Bam*HI; E, *Eco*RI; S, *Sac*I; K, *Kpn*I. Homologous recombination introduces an additional *Bam*HI site through the pgk neo cassette. (*B*) Southern blot hybridization analysis of *Bam*HI-digested ES cells and tail DNA from offsprings of $cgt^{+/-}$ intercrosses. neo probe is a 1.1-kb fragment; 3′-probe a 1.1-kb *Eco*RI fragment (3) coresponding to a genomic sequence downstream of the replacement sequence.

pGEM3Z using SP6 (BRL) or T7 RNA polymerase (Boehringer Mannheim) and [^{35}S]UTP. CGT antisense RNA and a sense probe as control were hybridized to 6–8 mm cryosections of brains of p20-24 mice that had previously been perfused in 4% paraformaldehyde in PBS and further processed as described (16). Bright field image was ×5.6.

CGT Enzyme Assay. CGT activity was determined as described (17) with synthetic D-2-hydroxyhexanoylsphingosine and UDP[^{14}C]galactose (Amersham) as substrates and microsomal protein of brain, liver and kidney from p18 wt and $cgt^{-/-}$ mice.

Lipid Analysis. Total lipid extracts of purified CNS myelin, sciatic nerve, liver, kidney, and spleen (1) of wt, hetero-, and homozygous CGT-deficient mice were homogenized in 10 volumes of chloroform-methanol (2:1 vol/vol) with an ultraturrax and centrifuged. The pellet was reextracted twice. The combined supernatants were taken to dryness under a stream of nitrogen. Lipids were dissolved in chloroform-methanol (2:1) to a final concentration of 20 mg/ml. Unsaponifiable sphingolipids were obtained by alkaline hydrolysis of total lipids. Aliquots were saponified in 1 ml of 0.5 N methanolic KOH at 37°C for 5 h. Water (1 ml) was added and the mixture extracted three times with chloroform. Phases were separated by centrifugation. The combined chloroform extracts were evaporated to dryness. Total and alkali-stabile lipids were separated on high-performance thin-layer chromatography plates using the solvent system chloroform/methanol/water, 65:25:4. Lipid bands were visualized by charring for phospholipids (18), glycolipids (19), sulfatides (20), and by charring for all lipid constituents with 50% H_2SO_4 at 120°C for 15 min. GalC and sGalC bands of wt and $cgt^{-/-}$ mice were separated by high-performance thin-layer chromatography, visualized by spraying with water, and scraped from plates. Individual lipids were extracted twice with chloroform/methanol (2:1), and aliquots were subjected to fast atom bombardment mass spectrometry and gas liquid chromatography.

Conduction Velocity Measurement. Nerve conduction was measured by proximal stimulation of the sciatic nerve at the knee and distal close to the hip, using a Medelec electromyograph, model MS92. Gait pattern was recorded as described (21, 22).

Electron Microscopy. Twenty-four-day-old mice were anesthetized with Nembutal and perfused with 3% glutaraldehyde and 2% paraformaldehyde in PBS via the left cardiac ventricle. Cervical segments of the spinal cord, optic, and sciatic nerve were obtained, postfixed in 1% phosphate-buffered OsO_4 in 0.1 M sucrose, and embedded in Epon 812. Ultrathin cross sections of spinal cord, optic, and sciatic nerve were contrasted with uranylacetate and lead citrate and examined as described (23).

RESULTS

We report here the generation of a CGT-deficient ($cgt^{-/-}$) mouse line by gene targeting (Fig. 1). Oligodendrocyte- and Schwann cell-specific gene expression relevant for myelination of axons was studied by Northern blot hybridization analyis (Fig. 2*A*). Expression of *cgt* was completely eliminated in the homozygous mutant mouse. No enhanced expression of any mRNA of the predominant myelin proteins MBP, proteolipid protein (PLP), MAG, and OMgp of oligodendrocytes, and MBP and P_0 of Schwann cells could be observed when normalized to the endogenous glyceraldehyde-phosphate dehydrogenase signal. *In situ* hybridization of horizontal sections of wt and $cgt^{-/-}$ brains with antisense CGT and MBP RNA also proved the absence of CGT mRNA in oligodendrocytes (Fig. 2*B*). The number of oligodendrocytes of wt and $cgt^{-/-}$ mice labeled with the *mbp* antisense RNA probe was similar, indicating a normal development of the oligodendrocyte lineage in the $cgt^{-/-}$ mutant mouse. Enzymatic activity of CGT was determined by the galactosyl transferase assay (17) (Fig. 2*C*). $cgt^{-/-}$ mice showed a complete loss of CGT activity in brain giving additional prove of the presence of only one CGT gene copy responsible for galactosphingolipid synthesis.

Oligodendrocytes and Schwann cells of the $cgt^{-/-}$ null mutant mouse produce a myelin membrane, the lipid bilayer of which is completely deficient in GalC and sGalC (Fig. 3). Total lipid extract and unsaponifiable lipids were separated and visualized with specific reagents. Two new glycolipid bands with R_f values intermediate between and below normal fatty acyl (nGalC) and hydroxy fatty acyl (hGal) and nsGalC, and hsGalC, respectively (see Fig. 3, arrows 1 and 2), occurred in the myelin lipid pattern of $cgt^{-/-}$ CNS and PNS. Mass spectroscopy identified the unknown lipids as hexosyl-substituted with *n*-saturated and α-hydroxylated very long chain fatty acid (18–26 C-atoms). Their sugar moiety was identified as a glucosyl derivative after acid hydrolysis, reduction and peracetylation as glucitol hexaacetate by GLC (not shown). Fatty acid analysis of these glucocerebrosides of $cgt^{-/-}$ mice proved that the ceramide intermediate, which is normally the precursor of the GalC synthesis in wt mouse, was utilized by a glucosyl transferase. These ceramide species were also utilized for sphingomyelin synthesis. The sphingomyelin band with lower R_f-value corresponds to long chain α-hydroxy fatty acid containing sphingomyelin (Fig. 3, arrow 3).

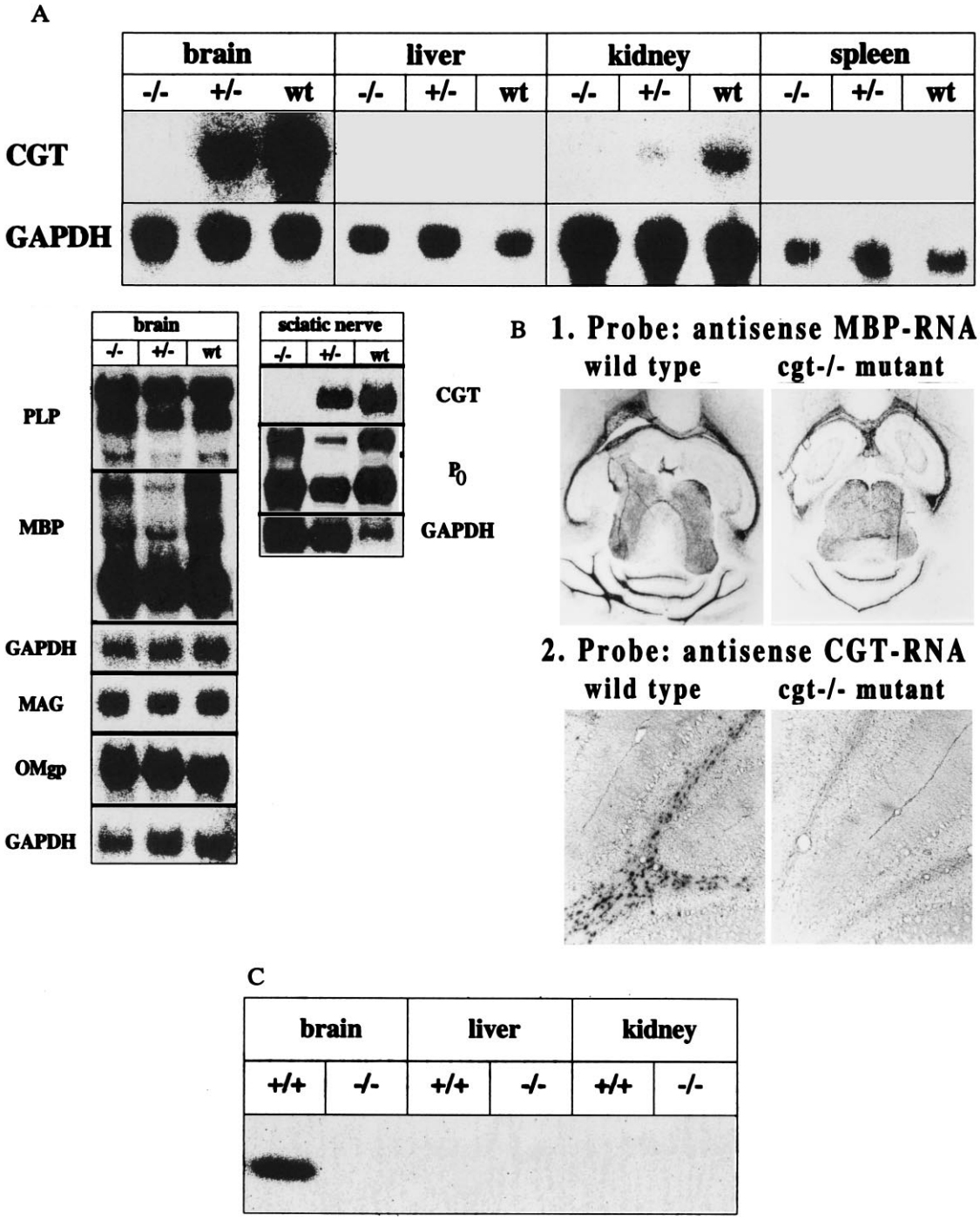

FIG. 2. Analysis of *cgt* expression and relevant myelin-associated genes of oligodendrocyte by Northern blot, *in situ* hybridization and enzyme assay. C57BL/6 mice were used as control mice in all comparative experiments. (*A*) Northern blot analysis of CGT, PLP, MBP, MAG, OMgp, and P_0 RNA of brain, liver, kidney, spleen, and sciatic nerve. Approximate sizes of transcripts: CGT, 3.2 kb; PLP, 1.6, 2.4 and 3.2 kb; MBP, 2.1 kb; MAG, 4 kb; OMgp, 1.8 kb; Po, 2.0 kb; glyceraldehyde-phosphate dehydrogenase, 1.2 kb. (*B*) Comparative *in situ* hybridization analysis of CGT and MBP expression in wt and homozygous $cgt^{-/-}$ mouse brain. (*C*) CGT activity of brain, liver and kidney of age matched p18-20 wt and homozygous mutant mice. Enzymatic activity was determined as described (17) with synthetic D-2-hydroxyhexanoylsphingosine and UDP[^{14}C]galactose (Amersham) as substrates and microsomal protein of brain, liver, and kidney from p18 wt and $cgt^{-/-}$ mice. The reaction product, radioactive [^{14}C]galactosyl ceramide, was detected in the lipid extract after separation by TLC as described and recorded with the phosphoimager. Only brain microsomes of wt mouse brain showed significant enzymatic activity, that of kidney was to weak to be detected by autoradiography.

Schwann cells also transfer a sulfate group to the newly formed glucocerebroside. These glucocerebrosides and their sulfate esters are unable to compensate the loss of galactosphingolipids. Although the ceramide component specific for GalC is utilized for the reduced synthesis of glucocerebrosides, the hydrophobic core of the bilayer and particularly the carbohydrate polar head group and charge pattern of the myelin membrane surfaces of the $cgt^{-/-}$ mouse remain seriously altered.

The complete loss of CGT activity in brain of myelinating homozygous $cgt^{-/-}$ mice gives additional prove of the presence of only one single ceramide galactosyl transferase gene copy responsible for oligodendrocyte-, Schwann cell-, and kidney-specific galactosphingolipid synthesis. The *in vivo* experiments

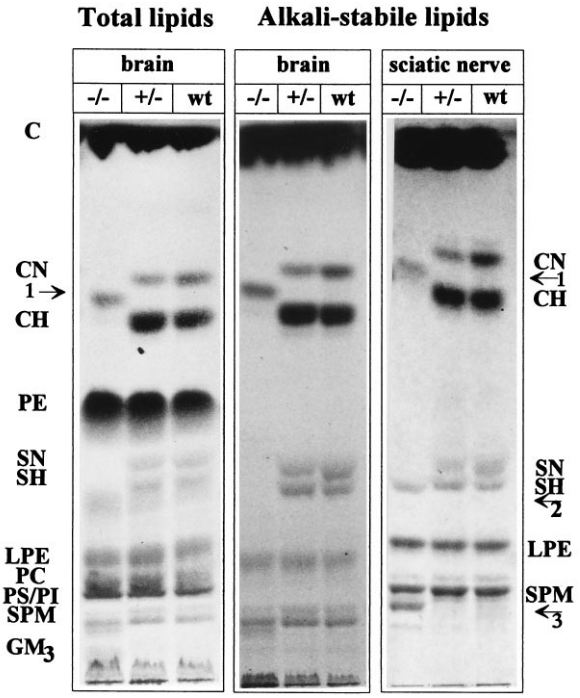

FIG. 3. Analysis of myelin lipids of brain and sciatic nerve of wt, hetero-, and homozygous $cgt^{-/-}$ mice (24-day-old). Brain, total and alkali-stable lipids; sciatic nerve, alkali-stable lipids; C, cholesterol; CN, normal fatty acid substituted GalC; CH, α-hydroxy fatty acid substituted GalC; PE, phosphatidylethanolamine; SN, normal fatty acid substituted sGalC; SH, α-hydroxy fatty acid substituted sGalC; LPE, lysophosphatidylethanolamine (lysoplasmalogens); PC, phosphatidylcholine; GM3, ganglioside GM3. Arrows: 1, glucocerebroside; 2, sulfated glucocerebroside; and 3, sphingomyelin-containing long chain α-hydroxy fatty acids.

indicate furthermore that cerebrosides and sulfatides are not primarily responsible and essential for the differentiation of the oligodendrocyte precursor cell.

The growth of the homozygous $cgt^{-/-}$ mice is retarded as shown in the comparison of wt and homozygous sibling (Fig. 4). Most of the homozygous mice have died by the end of the myelination period ≈p25-p30.

Electromyographic measurement of the conduction velocity of the sciatic nerve of age-matched wt and $cgt^{-/-}$ mice indicated that the velocity observed had decreased from 22–25 *m/s* in wt C57BL/6 to 4–8 *m/s* in $cgt^{-/-}$ mice (n = 6, 18–20 days old) which is that of unmyelinated axons (24) (Fig. 5*A*).

A whole body tremor of $cgt^{-/-}$ mice is observed after day 10–12 accompanied by increasing loss of locomotor activity and a very conspicuous gait pattern, as documented by the hind foot pattern (25), Fig. 5*B*. In the open field test the homozygous $cgt^{-/-}$ mutant mouse showed only minute activity. Furthermore, homozygotes were unable to perform the horizontal wire test (22) due to an increasing weakness of their front and hind legs, which were severely paralyzed around day 21. Heterozygous mice showed no neurological symptoms.

In electron microscopy the myelin sheath of CNS (optic nerve) and PNS (sciatic nerve) axons showed a regular periodicity of the main and intermediate dense lines in wt and $cgt^{-/-}$ mice (Fig. 6 *A–F*). This is surprising in view of the

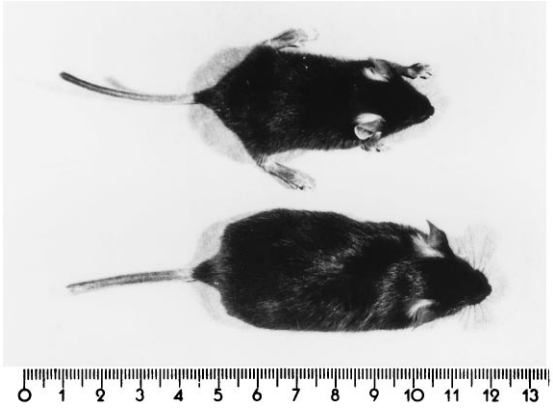

FIG. 4. Age-matched (p24) wt (*Lower*) and $cgt^{-/-}$ (*Upper*) mice showing the growth retardation of $cgt^{-/-}$ upper mouse. (Scale in cm.)

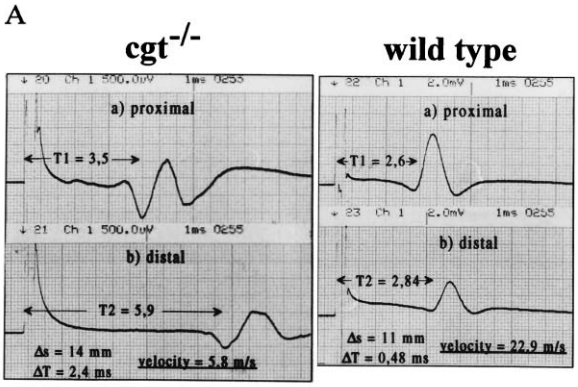

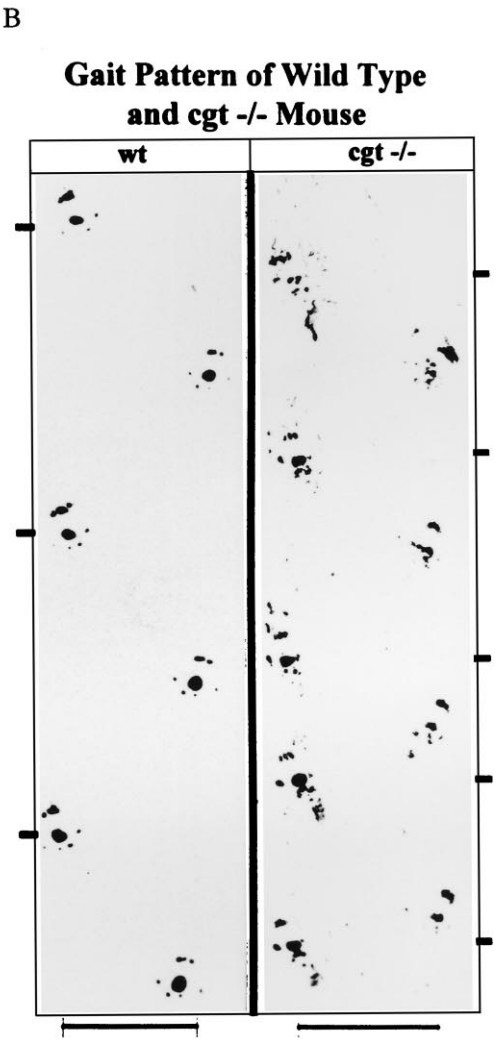

FIG. 5. (*A*) Nerve conduction velocity of $cgt^{-/-}$ is decreased from 22–25 *m/s* to 4–8 *m/s* when p18-20 mice were compared. (*B*) Gait pattern of wt and $cgt^{-/-}$ mouse.

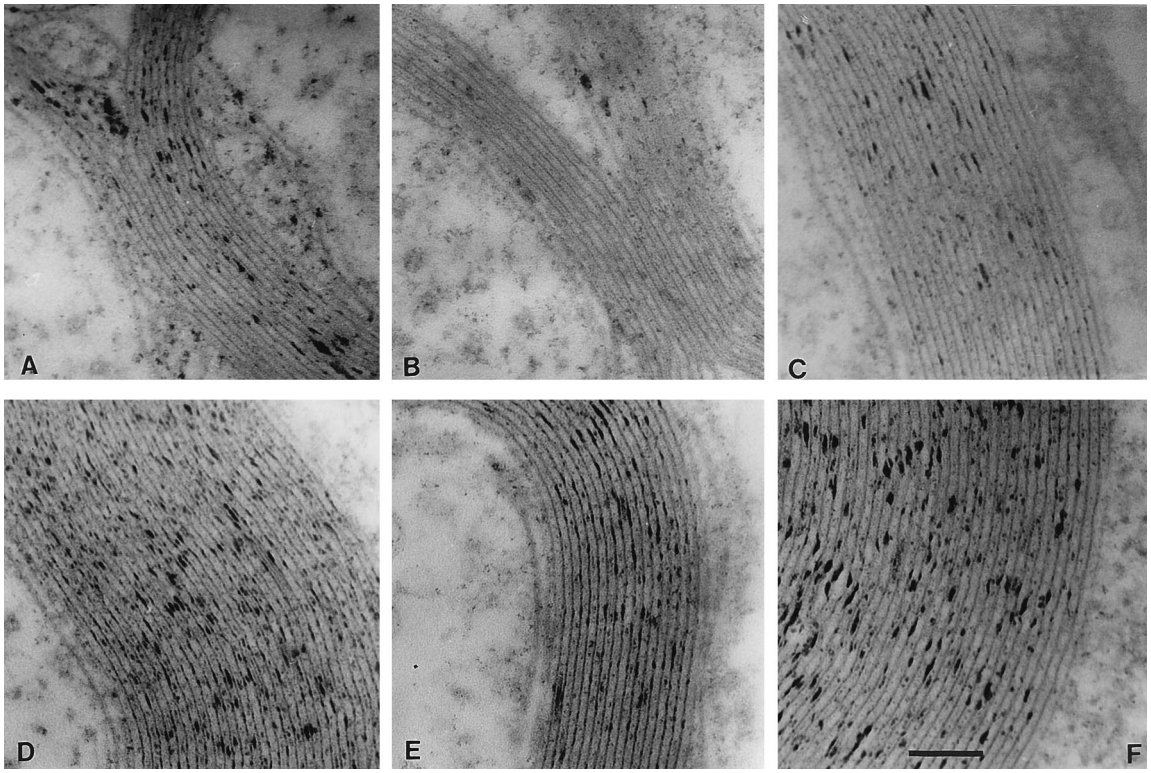

FIG. 6. Electron microscopy of cross sections of the optic and sciatic nerve of p24 wt, hetero- and homozygous mutant mice. (*A–C*) Optic nerve. Cross section of optic nerve of *A*, $cgt^{-/-}$; *B*, $cgt^{+/-}$; *C*, wt. (*D–F*) Sciatic nerve. Cross section of sciatic nerve of *D*, $cgt^{-/-}$; *E*, $cgt^{+/-}$; *F*, wt. (Bar = 1.0 mm.)

striking phenotype of the $cgt^{-/-}$ mutant comparable with the dysmyelinosis with severe hypomyelination seen in *shiverer*, *jimpy* mouse, or myelin-deficient rat.

These results indicate that although ultrastructurally the myelin membrane system of CNS and PNS is inconspicuous, the lipid bilayer structure on the molecular level must be severely altered by the lack of the membrane-stabilizing galactocerebrosides and sulfatides.

DISCUSSION

Pivotal for the insulator function of the myelin membrane structure of CNS and PNS and saltatory conduction of axons is the unperturbed lipid bilayer structure. Galactolipids GalC and sGalC contribute to the structure and stability of the myelin lipid bilayer on three levels. (*i*) The all-trans configuration of the long chain (C18–C26), mostly saturated and α-hydroxylated fatty acyl chains together with the alkane chain of the long chain sphingosine base contribute to the tight packing of the hydrophobic core domain. A high concentration of cholesterol and highly unsaturated ethanolamine plasmalogen adjusts its fluidity. (*ii*) The polar head groups of GalC and sGalC contribute significantly to the inner and outer membrane surface. sGalC together with the polar head groups of phosphatidylserine and -inositol (phosphates) provide a polyanionic surface array. Strong interactions with both the positively charged MBP at the cytosolic and hydrophobic domains of PLP at the extracytoplasmic surface might contribute to the tight compaction of the multilayer membrane system. (*iii*) At the interphase of the membrane the abundant galactosphingolipids contribute to a dense network of H-bonding between three β-hydroxy groups of cholesterol, the 3R hydroxy group of the sphingosine moiety of sphingolipid, the α-D-hydroxy groups of the acyl chains and the amide bond of the sphingolipids. It is likely though not proven that these interactions are concentrated at the extracytoplasmic surface of the myelin lipid bilayer. The cooperativity of these structures renders the lipid bilayer of myelin impermeable for ions, a prerequisite of its insulation properties.

In the null mutant $cgt^{-/-}$ mouse lack of GalC and sGalC in the lipid bilayer of myelin leaves cholesterol and highly unsaturated phospholipids as main constituents for the assembly of the lipid bilayer. Consequently the phase transition temperature of the lipid bilayer should be considerably lowered and membrane fluidity and permeability increased. The dramatically altered electrophysiology due to the structural changes in the lipid bilayer of CNS and PNS myelin membrane is apparent in the loss of insulating properties of the internodes and blocked saltatory conduction. The velocity of nerve conduction of the sciatic nerve of 24-day-old wt mice ($n = 6$) of 25–28 m/s was reduced in age matched homozygous $cgt^{-/-}$ mice to 4–8 m/s, comparable with that of unmyelinated axons (24) For nonmyelinated axons (1.1 μm diameter) originating from dorsal root ganglia a conduction velocity of 2.3 m/s has been measured. The saltatory conduction of homozygous $cgt^{-/-}$ mice has turned into the propagation of the action potential by continuous depolarization of the axon, due to the complete loss of the insulating properties of the multilayered internodal membrane system. Ectopic discharges along the axons of CNS and PNS block saltatory conduction and cause whole body tremor of the $cgt^{-/-}$ mouse similar to the homozygous *shiverer* mouse in which the myelination is fully down regulated. Rapidly developing paresis of the limbs and facial nerves monitors a demyelinating phenotype comparable with that observed in chronic peripheral neuropathies.

The structure-function relation of the main myelin proteins—the peripheral MBP, the integral PLP and MAG, synthesized by oligodendrocytes and P_0 by Schwann cells—is rapidly emerging now particularly from the natural MBP mutant *shiverer* 25, the null-allelic mouse mutants of PLP ($plp^{-/-}$) (26), ($plp^{-/-}$, $mbp^{-/-}$), MAG ($mag^{-/-}$) (27), and P_0 (28) generated by gene targeting with homologous recombination.

The *in vivo* analysis of the function of the GalC and sGalC constituents of the lipid bilayer of the myelin membrane of mammalian CNS and PNS is, to our knowledge, the first example which demonstrates the great potential of gene targeting by homologous recombination in studies addressing functional aspects of lipid structures in biological membranes.

The support by Dr. A. Walsh, Laboratory of Animal Research Center, Rockefeller University, New York, during the animal experiments is gratefully acknowledged. We thank Prof. Dr. Haupt, Neurologische Universitätsklinik Köln, for the electromyographic measurements, and Dr. G. Pohlentz, Physiologisch-Chemisches Institut, Universität Bonn, for mass spectroscopic analyses. This work was generously supported by the Deutsche Forschungsgemeinschaft, Grant SFB 243, project A4, (W.S.), and by the Alexander von Humboldt Foundation through the Max Planck Research Prize (W.S.).

1. Schulte, S. & Stoffel, W. (1993) *Proc. Natl. Acad. Sci. USA* **90,** 10265–10269.
2. Schulte, S. & Stoffel, W. (1995) *Eur. J. Biochem.* **233,** 947–953.
3. Bosio, A., Binczek, E. & Stoffel, W. (1996) *Genomics* **35,** 223–226.
4. Bosio, A., Binczek, E., Le Beau, M. M., Fernald, A. A. & Stoffel, W. (1996) *Genomics* **34,** 69–75.
5. Gard, A. L. & Pfeiffer, S. E. (1990) *Neuron* **5,** 615–625.
6. Raff, M., Mirsky, R., Fields, K., Lisak, R., Dorfman, S., Silberberg, D., Gregson, N., Leibowitz, S. & Kennedy, M. (1978) *Nature (London)* **274,** 813–816.
7. Raff, M., Fields, K., Hakomori, S., Mirsky, R., Pruss, R. & Winter, J. (1979) *Brain Res.* **174,** 383–308.
8. Raff, M., Abney, E. & Miller, R. (1984) *Dev. Biol.* **106,** 53–60.
9. Raff, M., Abney, E. & Fok-Seang, J. (1985) *Cell* **42,** 61–69.
10. Bansal, R. & Pfeiffer, S. E. M. (1989) *Proc. Natl. Acad. Sci. USA* **86,** 6181–6185.
11. Dyer, C. A. (1993) *Mol. Neurobiol.* **7,** 1–22.
12. Mansour, S., Thomas, K. & Capecchi, M. (1988) *Nature (London)* **336,** 348–352.
13. Kuehn, M. R., Bradley, A., Robertson, E. J. & Evans, M. J. (1987) *Nature (London)* **326,** 295–298.
14. Laird, P. W., Zijderveld, A., Linders, K., Rudnicki, M. A., Jaenisch, R. & Berns, A. (1991) *Nucleic Acids Res.* **19,** 4293.
15. Chomczynski, P. & Sacchi, N. (1987) *Anal. Biochem.* **162,** 156–159.
16. Ausubel, F. M., Brent, R., Kingston, R. E., Moore, D. D., Seidman, J. G., Smith, J. A. & Struhl, K. (1987) *Current Protocols in Molecular Biology* (Wiley, New York).
17. Neskovic, N., Roussel, G. & Nussbaum, J. (1986) *J. Neurochem.* **47,** 1412–1418.
18. Dittmer, J. & Lester, R. (1964) *J. Lipid Res.* **5,** 126–127.
19. Ledeen, R. W. & Yu, R. K. (1982) *Methods Enzymol.* **83,** 139–191.
20. Schnaar, R. L. & Needham, L. K. (1994) *Methods Enzymol.* **230,** 371–389.
21. Xu, M., Moratalla, R., Gold, L. H., Hiroi, N., Koob, G. F., Graybiel, A. M. & Tonegawa, S. (1994) *Cell* **79,** 729–742.
22. Wallace, E. J., Krauter, E. E. & Campbell, B. A. (1980) *J. Gerontol.* **35,** 364–370.
23. Büssow, H. (1978) *J. Neurocytol.* **7,** 207–214.
24. Gasser, H. S. (1950) *J. Gen. Physiol.* **33,** 651–690.
25. Aiba, A., Kano, M., Chen, C., Stanton, M. E., Fox, G. D., Herrup, K., Zwingman, T. A. & Tonegawa, S. (1994) *Cell* **79,** 377–388.
26. Boison, D. & Stoffel, W. (1994) *Proc. Natl. Acad. Sci. USA* **91,** 11709–11713.
27. Li, C., Tropak, M. B., Gerlai, R., Clapoff, S., Abramow-Newerly, W., Trapp, B., Peterson, A. & Roder, J. (1994) *Nature (London)* **369,** 747–750.
28. Giese, K. P., Martini, R., Lemke, G., Soriano, P. & Schachner, M. (1992) *Cell* **71,** 565–576.